

Inclusive and differential cross section measurements of $t\bar{t}b\bar{b}$ production in the lepton+jets channel at $\sqrt{s} = 13$ TeV

EMANUEL PFEFFER¹

ON BEHALF OF THE CMS COLLABORATION

*Institute for Experimental Particle Physics
Karlsruhe Institute of Technology, Germany*

Differential cross section measurements of the associated production of top quark and b quark pairs, $t\bar{t}b\bar{b}$, are presented. The results are based on data from proton-proton collisions collected by the CMS detector at the LHC at a centre-of-mass energy of $\sqrt{s} = 13$ TeV, corresponding to an integrated luminosity of 138 fb^{-1} . Four fiducial phase space regions are defined targeting distinct aspects of the $t\bar{t}b\bar{b}$ process. Kinematic variables are defined at the stable particle level and distributions are unfolded to the particle level through maximum likelihood fits. The cross sections are measured in the lepton+jets decay channel of the top quark pair, using events with exactly one isolated electron or muon and at least five jets. The results are compared with predictions from several event generators. The differential measurements have relative uncertainties in the range of 2–50%, depending on the phase space and the observable.

PRESENTED AT

16th International Workshop on Top Quark Physics
(Top2023), 24–29 September, 2023

¹Contact: emanuel.pfeffer@cern.ch

1 Introduction

The two widely separated energy scales of the top and the bottom quark, each with a very different, non-negligible mass, result in particular complexity when it comes to modeling processes in which both quark flavours occur simultaneously as pairs [1, 2]. These processes arise in proton-proton collisions at the CERN LHC as associated production of top and bottom quark-antiquark pairs, $t\bar{t}b\bar{b}$. Due to the different emerging energy scales, the measurement of these processes is a major test of perturbative quantum chromodynamics (QCD) calculations. In addition, a precise knowledge of $t\bar{t}b\bar{b}$ production is crucial in order to be able to understand other important processes for which $t\bar{t}b\bar{b}$ forms the leading irreducible background. Among these processes and searches are the measurement of the associated production of top quark pairs with Higgs bosons with the Higgs boson decaying into a pair of b quarks ($t\bar{t}H(b\bar{b})$) [3, 4], and measurements of the simultaneous production of four top quarks ($t\bar{t}t\bar{t}$) [5, 6]. Both processes directly access a key parameter of the Standard Model (SM), the top quark Yukawa coupling.

2 The CMS detector

The Compact Muon Solenoid (CMS) detector is an experiment at the CERN LHC with a superconducting solenoid reaching a high magnetic field of 3.8 T. An all-silicon pixel and strip tracker is positioned as close as possible to the beam axis. The trackers are surrounded by a lead-tungstate scintillating-crystals electromagnetic calorimeter, and followed by a brass-scintillator sampling hadron calorimeter. All these components are located inside the solenoid. Outside the magnet the iron yoke of the flux-return is combined with muon detectors. This onion-like construction allows almost every spatial angle to be covered so that as much of the collision as possible may be reconstructed and recorded. A two-staged trigger system is employed for the recording in order to be able to handle the resulting data volume of over 40 million collisions per second. Only after the calculation by a processor farm of the second tier it is possible to store the collected data [7].

3 Modelling approaches

In the analysis, six different modelling approaches for $t\bar{t}b\bar{b}$ production are compared with the measurements. These approaches differ in the Monte Carlo (MC) event generators used, the processes simulated at the matrix-element (ME) level, the applied parton showering (PS) models, the scales used and additional parameters which can be found in [8]. The main difference between the simulations, apart from the settings mentioned before, is the simulated process at ME level. Most importantly,

a distinction can be made between models using a $t\bar{t}$ simulation at the ME level at next-to-leading order (NLO) accuracy in QCD and models using $t\bar{t}b\bar{b}$ at the ME level at NLO. Two of the tested models describe $t\bar{t}$ at the ME level, three others test $t\bar{t}b\bar{b}$ at ME level and one simulation describes $t\bar{t}$ +jets with up to two additional jets at ME level. All the simulation approaches are summarized in Table 1.

Table 1: Generator settings for all considered modeling approaches of $t\bar{t}b\bar{b}$ production. The top quark mass value is set to $m_t = 172.5$ GeV, and in cases where a massive b quark is defined, the mass is set to $m_b = 4.75$ GeV. The transverse mass is defined as $m_{T,i} = \sqrt{m_i^2 + p_{T,i}^2}$ and used to calculate the scalar sum $H_T = \sum_{i=t,\bar{t},b,\bar{b},g} m_{T,i}$. The POWHEG specific h_{damp} value is given for the first three generator setups, all others do not use this parameter and are therefore marked with (N/A) [8].

Generator setup	Process/ ME order	Generator/ Shower	Tune	PDF set	h_{damp}	Scales
POWHEG+P8 $t\bar{t}$ 5FS	$t\bar{t}$ / NLO	POWHEG v2/ PYTHIA 8.240	CP5	5FS NNP3.1 NNLO	$1.379m_t$	$\mu_F = \mu_R = m_{T,t}$
POWHEG+H7 $t\bar{t}$ 5FS	$t\bar{t}$ / NLO	POWHEG v2/ HERWIG 7.13	CH3	5FS NNP3.1 NNLO	$1.379m_t$	$\mu_F = \mu_R = m_{T,t}$
POWHEG+OL+P8 $t\bar{t}b\bar{b}$ 4FS	$t\bar{t}b\bar{b}$ / NLO	POWHEG-BOX-RES/ PYTHIA 8.240	CP5	4FS NNP3.1 NNLO as 0118	$1.379m_t$	$\mu_R = \frac{1}{2} \prod_{i=t,\bar{t},b,\bar{b}} m_{T,i}^{1/4}$, $\mu_F = H_T/4$
SHERPA+OL $t\bar{t}b\bar{b}$ 4FS	$t\bar{t}b\bar{b}$ / NLO	SHERPA 2.2.4	SHERPA	4FS NNP3.0 NNLO as 0118	N/A	$\mu_R = \prod_{i=t,\bar{t},b,\bar{b}} m_{T,i}^{1/4}$, $\mu_F = H_T/2$
MG5_aMC+P8 $t\bar{t}b\bar{b}$ 4FS	$t\bar{t}b\bar{b}$ / NLO	MADGRAPH5_aMC@NLO v2.4.2/PYTHIA 8.230	CP5	4FS NNP3.1 NNLO as 0118	N/A	$\mu_F = \mu_R = \sum m_T$
MG5_aMC+P8 $t\bar{t}$ +jets FxFX $t\bar{t}$ +jets FxFX 5FS	$t\bar{t}$ +jets FxFX/ NLO [≤ 2 jets]	MADGRAPH5_aMC@NLO v2.6.1/PYTHIA 8.240	CP5	5FS NNP3.1 NNLO	N/A	$\mu_F = \mu_R = \sum m_T$, qCut = 40 GeV, qCutME = 20 GeV

4 Phase space regions and observables

Four different phase space regions are defined, which specifically examine different facets of $t\bar{t}b\bar{b}$ production. These are partially overlapping and therefore not orthogonal. The first region requires at least five jets with at least three of them being b jets (“ ≥ 5 jets: $\geq 3b$ ”). This is the most inclusive of all the regions considered and takes into account that one of the expected jets may be located outside the acceptance region. A second region, labeled as “ ≥ 6 jets: $\geq 4b$ ”, targets fully resolved $t\bar{t}b\bar{b}$ events and requires at least six jets of which at least four must be b jets. Two additional regions focus on the additional radiation of further light-flavour (i.e. non b) jets, these demand at least six (seven) jets, at least three (four) b jets and at least three light-flavour jets and are labeled as “ ≥ 6 jets: $\geq 3b, \geq 3$ light” (“ ≥ 7 jets: $\geq 4b, \geq 3$ light”). Each of these four fiducial phase space regions additionally requires exactly one electron or muon. Jets considered must meet $p_T > 30$ GeV and $|\eta| < 2.4$ thresholds. All

detailed specifications for object and event reconstruction, particle level definitions as well as event selection can be found in [8]. Together with the inclusive cross section for all four regions previously described, a total of 37 different observables are defined. Four of these normalized differential cross section distributions are discussed in Section 5.

5 Normalized differential cross sections

Two of the observables in the “ ≥ 6 jets: $\geq 4b$ ” region discussed below are based on the definition of the pair of b jets which have the smallest spatial separation in the (η, ϕ) -plane. For this, every possible b jet combination is calculated according to

$$\Delta R_{bb} = \sqrt{(\Delta\eta_{bb})^2 + (\Delta\phi_{bb})^2} \quad . \quad (1)$$

The b jet pair with the smallest spatial distance ΔR_{bb} is then labeled as bb^{extra} in the following. With this methodology, the b jets determined in this manner are the two additional b jets that do not originate from the top quark decay in 49% of the events in the phase space under scrutiny [8]. In this way, observables with properties expected to be sensitive to the modeling of the gluon splittings to bb are considered. The two observables defined on this basis are the spatial distance ($\Delta R(bb^{\text{extra}})$) and the invariant mass of the bb pair ($m(bb^{\text{extra}})$). The distributions of these observables are shown in Figure 1. It can be seen that the distribution of the spatial distance $\Delta R(bb^{\text{extra}})$ for the simulations POWHEG+OL+P8 $t\bar{t}b\bar{b}$ 4FS and SHERPA+OL $t\bar{t}b\bar{b}$ 4FS agree quite well with data in this observable. In contrast, the modeling approach POWHEG+P8 $t\bar{t}$ 5FS shows distances ΔR that are too large. This cannot simply be attributed to the different calculation at ME level, as the POWHEG+H7 $t\bar{t}$ 5FS model also shows a deviation, but with an opposite trend towards too small distances $\Delta R(bb^{\text{extra}})$. This observable is mainly driven by the PS, which is different in both $t\bar{t}$ modeling approaches. This indicates that the different PS configurations are not optimally tuned in this observable. The deviating behavior of the event simulation in this crucial observable can also be seen in the $t\bar{t}b\bar{b}$ modeling performed in the context of the LHC Higgs Working Group [9]. The behavior of the distribution of the invariant mass of the bb^{extra} pair is similar to the distance $\Delta R(bb^{\text{extra}})$. Here, the simulations POWHEG+OL+P8 $t\bar{t}b\bar{b}$ 4FS and SHERPA+OL $t\bar{t}b\bar{b}$ 4FS describe the invariant mass quite well compared to the measured data, while the modeling approach POWHEG+H7 $t\bar{t}$ 5FS tends to predict invariant masses that are too small.

Another interesting observable is the average spatial distance ΔR of all b jets in an event, $\Delta R_{bb}^{\text{avg}}$. Such an observable is used, for example, in $t\bar{t}H(b\bar{b})$ analyses as an helpful input feature for artificial neural networks in the separation of signal and backgrounds [4]. In Figure 1 (lower left) it can be seen that all modeling approaches examined tend to deliver on average $\Delta R_{bb}^{\text{avg}}$ values that are too large compared to

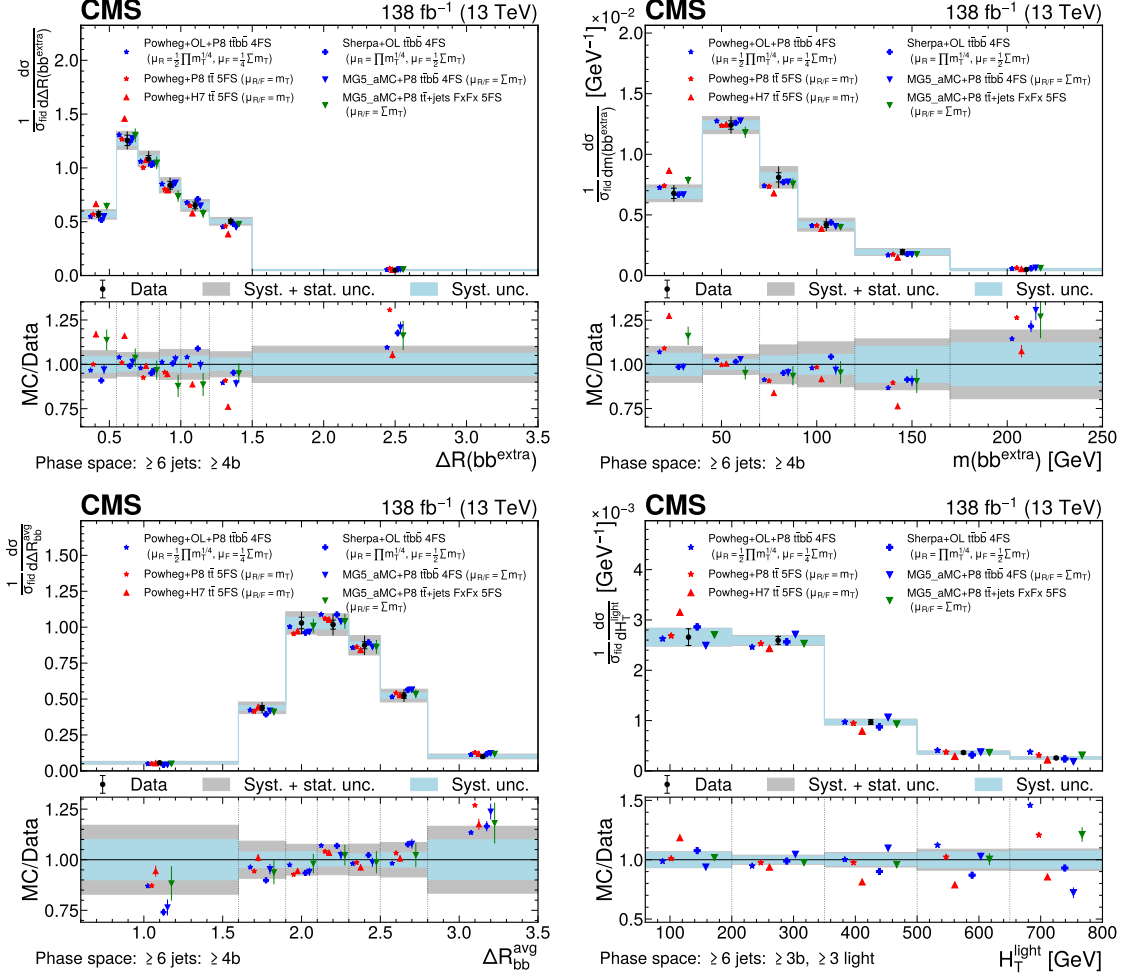


Figure 1: Predicted and observed normalized differential cross sections in the ≥ 6 jets: $\geq 4b$ fiducial phase space, for the ΔR (upper left), invariant mass (upper right) of the extra b-jet pair (bb^{extra}), average $\Delta R_{\text{bb}}^{\text{avg}}$ of all b jets in an event (lower left), and the scalar p_T sum of all light jets H_T^{light} in the ≥ 6 jets: $\geq 3b$, ≥ 3 light phase space. Data represented by points. Inner (outer) vertical bars as well as blue (grey) bands are indicating the systematic (total) uncertainties. The predictions include their statistical uncertainties due to limited number of simulated events [8].

data. However, it should be noted that the uncertainties of the measurement are still large, such that the trend is not (yet) very significant and mainly statistically limited.

An observable that probes the additional light-flavour jet radiation is the scalar p_T sum of all light-flavour jets in the ≥ 6 jets: $\geq 3b, \geq 3$ light phase space. The normalized differential cross section is shown in Figure 1 (lower right). This observable reveals that the prediction of H_T^{light} in the POWHEG+OL+P8 $t\bar{t}b\bar{b}$ 4FS modeling approach is mis-modeled compared to the measured data since the p_T of the light jets tends to be predicted too large. On the other hand, in the POWHEG+H7 $t\bar{t}$ 5FS modeling approach the p_T of the light-flavour jets is rather soft. All other event simulations examined show a tendency to describe this observable more accurately.

Important parameters for $t\bar{t}b\bar{b}$ simulations at the ME level are the renormalization and factorization scales μ_R and μ_F . Various nominal models are used by the ATLAS and CMS Collaborations and are compared in [9]. Therefore, it is important to check variations of μ_R, μ_F and their effect on distributions depending on the choice of both scales. These scales are independently varied by a factor of 2 and 0.5 and the corresponding re-weighted distributions of the POWHEG+OL+P8 $t\bar{t}b\bar{b}$ 4FS modeling approach are examined. This is shown for the H_T^{light} observable in the ≥ 6 jets: $\geq 3b, \geq 3$ light phase space in Figure 2.

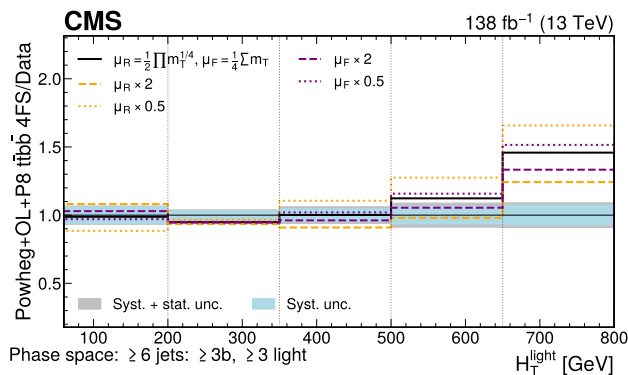


Figure 2: POWHEG+OL+P8 $t\bar{t}b\bar{b}$ 4FS modeling approach with varied μ_R and μ_F scale settings as a ratio of normalized differential cross section predictions to the measured normalized differential cross sections for H_T^{light} in the ≥ 6 jets: $\geq 3b, \geq 3$ light phase space. The systematic (total) uncertainties of the measurement are represented as blue (grey) bands. Variations of the μ_R (μ_F) scale relative to the nominal scale setting are shown in orange (purple) [8].

In the ratio of the predictions with varied scale settings to the measured data it can be observed that a larger choice of both scales would be preferred by the data in this particular observable. This suggests the prediction of light-flavor jets with preferably large transverse momenta may not necessarily be a problem of the generator, instead

it could be necessary to optimize the choice of scales being applied. Similar trends are observed for other observables, as discussed in [8].

6 Summary

Normalized differential cross section measurements of the associated production of top quark-antiquark and bottom quark-antiquark pairs for events with precisely one electron or muon have been presented. These measurements are based on recorded data from proton-proton collisions by the CMS experiment at $\sqrt{s} = 13$ TeV and a corresponding to an integrated luminosity of 138 fb^{-1} [8]. Multiple observables are defined targeting b jets as well as additional light jet radiation produced in association with top quark pairs. The relative uncertainties range from 2–50% depending on the phase space and the observable. None of the modeling approaches examined simultaneously describe all measured differential distributions in all phase space regions. Thus, depending on the phase space and observable, mis-modeling is still evident and optimization is necessary for a more accurate description of the observed processes. A Rivet routine is available for tuning new modeling approaches [10].

ACKNOWLEDGEMENTS

This research was supported by the German Federal Ministry of Education and Research (BMBF) under grant 05H21VKCCB. I would like to express my gratitude for BMBF's financial support.

References

- [1] F. Buccioni et al. NLO QCD predictions for $t\bar{t}b\bar{b}$ production in association with a light jet at the LHC. *JHEP*, 12:015, 2019. [https://doi.org/10.1007/JHEP12\(2019\)015](https://doi.org/10.1007/JHEP12(2019)015).
- [2] T. Ježo et al. New NLOPS predictions for $t\bar{t}+b$ -jet production at the LHC. *Eur. Phys. J. C*, 78:502, 2018. <https://doi.org/10.1140/epjc/s10052-018-5956-0>.
- [3] ATLAS Collaboration. Measurement of Higgs boson decay into b-quarks in associated production with a top-quark pair in pp collisions at $\sqrt{s} = 13$ TeV with the ATLAS detector. *JHEP*, 06:97, 2022. [http://dx.doi.org/10.1007/JHEP06\(2022\)097](http://dx.doi.org/10.1007/JHEP06(2022)097).

- [4] CMS Collaboration. Measurement of the cross section for $t\bar{t}$ production with additional jets and b jets in pp collisions at $\sqrt{s} = 13$ TeV. *JHEP*, 07:125, 2020. [https://doi.org/10.1007/JHEP07\(2020\)125](https://doi.org/10.1007/JHEP07(2020)125).
- [5] ATLAS Collaboration. Observation of four-top-quark production in the multilepton final state with the ATLAS detector. *Eur. Phys. J. C*, 83:496, 2023. <https://doi.org/10.1140/epjc/s10052-023-11573-0>.
- [6] CMS Collaboration. Observation of four top quark production in proton-proton collisions at $\sqrt{s} = 13$ TeV. *Physics Letters B*, 847:138290, 2023. <https://doi.org/10.1016/j.physletb.2023.138290>.
- [7] CMS Collaboration. The CMS experiment at the CERN LHC. *Journal of Instrumentation*, Aug 2008. <https://doi.org/10.1088/1748-0221/3/08/S08004>.
- [8] CMS Collaboration. Inclusive and differential cross section measurements of $t\bar{t}b\bar{b}$ production in the lepton+jets channel at $\sqrt{s} = 13$ TeV. <https://arxiv.org/abs/2309.14442>, 2023. Submitted to *JHEP*.
- [9] L. Ferencz et al. Study of $ttbb$ and ttW background modelling for ttH analyses. <https://arxiv.org/abs/2301.11670>, 2023.
- [10] CMS Collaboration. Inclusive and differential cross section measurements of $t\bar{t}b\bar{b}$ production in the lepton+jets channel at $\sqrt{s} = 13$ TeV (Version 1). HEPData (collection), 2023. <https://doi.org/10.17182/hepdata.138416.v1>.